

Temporal Behavior of the Ion Velocity Distribution Functions in Pulsed Helicon Plasma Sources

IEPC-2005-309

*Presented at the 29th International Electric Propulsion Conference, Princeton University,
October 31 – November 4, 2005*

Costel Biloiu^{*}, Xuan Sun[†], and Earl Scime[‡]
West Virginia University, Morgantown, West Virginia, 26506, USA

Edgar Choueiri[§] and Rostislav Spektor^{**}
Department of Mechanical and Aerospace Engineering, Princeton University, Princeton, New Jersey, 08544, USA

Abstract: The temporal behavior of parallel and perpendicular ion velocity distribution functions (ivdf) in a pulsed, helicon-generated, expanding, argon plasma is presented. The ivdf's temporal evolution during the pulse was determined with time resolved (1 ms resolution), laser induced fluorescence (LIF). The parallel ivdf measurements indicate that, in the expansion region of the plasma and for certain operational parameters, two ion populations exist: a population moving at supersonic speeds (1.1 Mach) resulting from acceleration in an electric double layer (EDL) and a slow moving population (0.7 Mach) generated by local ionization. After 100 ms, although present, the EDL is not fully developed and has not reached steady state. Measurements of the perpendicular ivdf indicate constant radial expansion, with ion speeds of ≈ 400 m/s, in the expansion region.

Nomenclature

ν_0	=	rest frame absorption frequency
ν	=	Doppler-shifted absorption frequency
$\Delta\nu_{1/2}$	=	full width at half maximum (FWHM) of Doppler-broadened ion velocity distribution
\mathbf{v}	=	particle velocity
\mathbf{k}_L	=	laser propagation direction
c	=	speed of light
T_e	=	electron temperature
n_e	=	electron density
k_B	=	Boltzmann constant
e	=	elementary charge
λ_D	=	Debye length
Φ	=	space-charge induced potential drop
c_s	=	ion sound speed
γ	=	coefficient of isothermal expansion

^{*} Associate Researcher, Department of Physics, costel.biloiu@mail.wvu.edu

[†] PhD Student, Department of Physics, xsun@mix.wvu.edu

[‡] Professor, Department of Physics, escime@wvu.edu

[§] Professor, Department of Mechanical and Aerospace Engineering, choueiri@princeton.edu.

^{**} PhD Student, Department of Mechanical and Aerospace Engineering, rspektor@princeton.edu.

I. Introduction

HIGH plasma densities generated at low pressure and relatively modest input power (200W – 2 kW) make the helicon plasma source suitable for a wide range of applications. Plasma thrusters, as an alternative to chemical propulsion, are a relatively new application. For a thruster, the ejected plasma flux and the ion flow velocity are the critical source parameters. Large amounts of ion production by a helicon source and subsequent ion heating in an ion cyclotron cell comprise the key elements of the Variable Specific Impulse Magnetoplasma Rocket (VASIMR) plasma thruster concept. To create thrust, VASIMR relies on rf plasma heating and plasma acceleration in a magnetic nozzle.¹ Another promising application of helicon sources to propulsion involves energizing the ions exiting the source through a non-resonant nonlinear ion acceleration mechanism that involves beating electrostatic waves.² Recently, three different helicon source experiments have shown that at the open end of a helicon source connected to a larger expansion chamber, an electric double layer (EDL) can spontaneously form.³⁻⁵ Since the EDL accelerates and then ejects ions at supersonic speeds, this phenomenon could provide a simple means of turning a helicon source into a plasma thruster. Argon ions exit speeds between 8 and 15 km/s, i.e., few times the ion acoustic speed, have been reported.^{5,6} Pulsing the helicon discharge might solve some important thruster application issues such as plasma detachment or turbulent cross-field diffusion (as observed in magnetic nozzles). Studies on the Mini-Magnetic Plasma propulsion (M2P2) prototype for pulse lengths from one millisecond to several seconds showed an increase in plasma density for pulse length of 1 ms.⁷ The High Power Helicon (HPH) experiment reported plasma densities of $\approx 10^{14}$ cm⁻³ for 10 kW input power and a 200 μ s pulse length.⁸ Therefore, for thruster applications, an understanding of the time evolution of the ivdf is needed to choose the optimal operational parameters (duty cycle, pulse length, input power, driving frequency) for the desired specific impulse along the expansion direction while minimizing the ion energy in the perpendicular direction.

In this work, we investigate the temporal behavior of the parallel and perpendicular ion velocity distribution functions (ivdf) in argon plasma in two pulsed helicon sources. The ivdf temporal evolution during the pulse was obtained with a time and velocity resolved laser induced fluorescence (LIF) technique. The only modification to the experimental apparatus we typically use for LIF measurements in steady-state plasmas is the addition of a digital oscilloscope on which the LIF emission versus time is averaged over many tens of pulses.⁹ Time resolution of 1 ms is sufficient to investigate ion heating by pulsed beat-wave¹⁰ and electrostatic ion-cyclotron waves¹¹ heating in helicon sources and formation of ion beams in pulsed expanding helicon source plasmas.¹² We note that other researchers have used similar techniques to investigate externally imposed, repetitive, transient phenomena in a steady-state background plasma, e.g., the interaction between ions and ion cyclotron waves in argon plasmas.¹³ However, those experiments examined only the time-averaged interaction of the ions with the waves.

II. Helicon Plasma Sources

A. The HELIX Helicon Plasma Source

The HELIX (Hot hELIcon EXperiment) at West Virginia University consists of a 61 cm long, 10 cm diameter Pyrex tube mated coaxially with a 91 cm long, 15 cm diameter stainless steel tube. Ten electromagnets produce a magnetic field of 0 – 1.2 kG along the tube axis. A 19 cm long, half wave, $m = +1$, helical antenna couples the rf energy into the plasma. A rf power supply and tunable matching network furnishes up to 2 kW over a frequency range of 6 – 18 MHz. Switching between continuous wave mode and pulsed mode, as well as changing the pulse duty cycle, is accomplished with a pulse generator that modulates the rf source. The plasma produced in the source expands into a 4 m long 2 m in diameter aluminum diffusion chamber, LEIA (Large Experiment on Instabilities and Anisotropies). The LEIA expansion chamber is surrounded by 7 electromagnets that provide an axial magnetic field of 0 – 150 G. Therefore, under typical operating conditions, in the region between the helicon source and the expansion chamber there exists an axial magnetic field gradient of nearly 1 kG/m over a distance of about 0.7 m. Under typical working conditions in the steady-state mode for argon gas, electron temperatures and densities in HELIX are $T_e \approx 12 - 4$ eV and $n \approx 10^{11} - 10^{13}$ cm⁻³ while in LEIA $T_e \approx 7 - 2$ eV and $n_e \approx 1 \times 10^9 - 5 \times 10^{11}$ cm⁻³ as measured with rf compensated Langmuir probes¹⁴ and a swept frequency microwave interferometer.¹⁵

B. The BWX Helicon Plasma Source

The Beating Wave eXperiment (BWx) in the Princeton Electric Propulsion Laboratory consists of a small Pyrex cylinder, 6 cm in diameter, 37 cm in length, concentrically connected through an electrically floating aluminum plate to a large Pyrex cylinder 20 cm in diameter and 46 cm in length. At the other end of the small cylinder is a molybdenum plate that is electrically floating to minimize sputtering effects. The large cylinder is terminated with

an aluminum plate, also electrically floating. Five electromagnets provide an axial magnetic field of up to 1 kG. A 13 cm long Boswell saddle antennae wrapped around the small cylinder, 8 cm away from the junction between the chambers is used to create the plasma. The antennae is made from 6.35 mm copper tubing to allow water cooling and is fed by an 13.56 MHz rf power supply able to furnish up to 1.2 kW forward power through a L-type matching network. The rf power is modulated with a pulse generator with adjustable pulse length and duty cycle. Under typical operating parameters, $P = 500$ W, $B = 800$ G, and $p = 1$ mTorr in argon gas, the on-axis electron temperature and density in the large cylinder are $T_e \approx 3$ eV and $n_e \approx 10^{13}$ cm⁻³, respectively.

III. Laser Induced Fluorescence (LIF) for pulsed argon plasmas

In a steady-state plasma, a LIF measurement is a measurement of the time averaged velocity distribution. Weak LIF emission from a steady-state plasma can be detected in the presence of intense background light by modulating the probing laser beam and employing phase synchronous detection, i.e., using a lock-in amplifier. Pulsed plasmas present the additional challenge of requiring time resolution while still detecting weak LIF emission. The minimum time resolution of a LIF measurement is set by the lifetime of the upper quantum level of the pumped transition, usually on the order of a few nanoseconds. Therefore, all repetitive phenomena with a characteristic time larger than a few nanoseconds could be investigated by LIF. In practice, however, time resolution is limited by the need to collect a sufficient number of LIF emission photons for reasonable signal to noise; the RC time constants of cables; the signal acquisition time requirements of the available electronics; and the particular plasma conditions. When the properties of the measurement electronics are well known, it is possible to improve the time resolution of LIF measurements by reducing the distorting effects of the electronics by digital signal processing.¹⁶ In the following, a simple LIF method based on lock-in detection and a digital oscilloscope averaging is presented. The temporal resolution of the method described in this work is limited to 1 ms by the integration time of the lock-in amplifier and the 1 ms update rate of the lock-in output electronics. Therefore it is suitable for temporal investigations of particle velocity distribution functions in pulsed discharges having pulse “on” times longer than few milliseconds. If higher time resolution is required, more sophisticated signal acquisition methods must be employed. By using boxcar integrators/averagers or multichannel scalers, time resolutions as high as few μ s can be obtained.¹⁷⁻¹⁹

For a Maxwellian distribution of particle velocities, the bulk flow velocity is obtained from the Doppler shift in the fluorescence spectrum

$$\nu = \nu_0(1 - \mathbf{v} \cdot \mathbf{k}_L / c) \quad (1)$$

where $\mathbf{v} \cdot \mathbf{k}_L$ is the particle velocity along the laser propagation direction. If Doppler broadening dominates over other line-broadening mechanisms, the temperature of the particle ensemble is inferred from the full width at half-maximum of the fluorescence line

$$k_B T = (mc^2 / 8 \ln 2)(\Delta \nu_{1/2} / \nu_0)^2 \quad (2)$$

For parallel argon ion LIF in HELIX, we used a LIF scheme in which the Ar II $3d' \ ^2G_{9/2}$ metastable state is optically pumped by 611.66 nm (vacuum wavelength) laser light to the $4p' \ ^2F_{7/2}^0$ state. The $4p' \ ^2F_{7/2}^0$ state decays to $4s' \ ^2D_{5/2}$ state by emission of 461.09 nm photons. The laser used is a single-mode tunable ring dye laser pumped by a 6 W argon-ion laser which yields about 200 mW of output power. A schematic of the LIF system used for parallel ivdf measurements in pulsed helicon plasma is shown in Fig. 1. After passing through a 10% beam splitter, the laser beam is modulated with a mechanical chopper at 4 kHz and then coupled into a multimode, non-polarization preserving, fiber optic cable. For parallel injection of laser light (to measure the parallel ivdf), a collimating lens, a Galilean telescope for beam waist reducing, followed by a linear polarizer-quarter wave plate combination for conversion of the unpolarized laser light exiting the fiber optic cable into circularly polarized light are used. The collimated injection beam has a diameter of 5 mm and a power of about 40% of the power exiting the fiber optic cable. With the laser light of a single circular polarization injected along the source axis, only one of the two σ transitions, specifically the $\Delta M = +1$ transition, is optically pumped. The 10% portion of the laser beam is passed through an iodine cell for a consistent zero velocity reference measurement to compensate for laser drift. Spontaneous emission from the iodine cell absorption lines is recorded with a photodiode for each scan of the dye laser wavelength. The fluorescence radiation is collected at 90° with respect to the laser beam by a collection optics assembly. The overlapping 5 mm diameter laser beam and 0.8 mm diameter collection focus spot yield a measurement volume of ≈ 4 mm³. Light exiting the collection fiber passes through a 1-nm band pass interference filter centered at 461 nm. Following the filter is a PMT detector with an integrated 20 kHz bandwidth pre-amplifier.

The PMT signal is composed of fluorescence radiation, electron impact induced radiation and electronic noise. A lock-in amplifier, referenced to the modulation signal from the mechanical chopper, is used to isolate the LIF signal from background emission at the fluorescence wavelength. Lock-in amplification is indispensable since the electron-impact induced emission is several orders of magnitude larger than the fluorescence signal. The signal from the lock-in amplifier is sent to one channel of a digital oscilloscope. Another channel records the pulsed waveform from the function generator used to drive the pulsed helicon discharge. The parallel drift velocity of the ions along the laser path is determined from the shift of the LIF peak relative to the iodine signal after correcting for the Zeeman shift of the σ absorption line as the laser is swept over 15 GHz. The experimental uncertainty in the ion flow speed is less than 50 m/s. Since Doppler broadening dominates the width of the measured ivdf, the parallel ion temperature is obtained from FWHM of the distribution according to Eq. (2).

For the BWX experiments, we used a tunable diode laser Sacher Lasertechnik model Lynx-TEC100 with an external Littrow cavity. The 8 GHz mode hop free range of the diode laser is large enough to span the absorption linewidth for 0.5 eV Ar ions. With the diode laser we used a three level argon LIF scheme proved to provide good signal to noise ratio for a wide range of plasma conditions.^{20,21} In this LIF scheme, the $3d\ ^4F_{7/2}$ Ar II metastable level is optically pumped to the $4p\ ^4D_{5/2}$ level by a diode laser tuned at 668.61 nm (vacuum wavelength) which decays to $4s\ ^4P_{3/2}$ by emitting fluorescence radiation at 442.72 nm. The tunable diode laser is comprised of a piezoelectric transducer controller (PZT) grating with a beam correction mirror. The laser controller in conjunction with a National Instruments I/O card, a Burleigh WA-1500 wavemeter, and LabWindows software are used to sweep the PZT voltage and thereby scan the laser wavelength through the absorption line over 8 GHz. Although the laser power varies slightly during such extended scans, distortion of the measured LIF emission lineshape are corrected by monitoring the laser power with a laser power meter at each laser frequency and then normalizing the LIF spectrum by the measured laser power. Instead of using an iodine cell, with the diode laser we used a wavemeter for real-time wavelength monitoring. During LIF measurements, the scan rate of the laser wavelength is limited by the 1 Hz update rate of the wavemeter. The laser power after the beam splitter is approximately 15 mW. After the beam splitter, the laser light is steered into the plasma, perpendicular to the magnetic field, with a pair of alignment mirrors. The laser polarization axis is chosen parallel to the magnetic field avoiding in this way, the pump of the Zeeman split σ lines. The internal Zeeman splitting of the remaining six linearly polarized π lines ($\Delta M_J = 0$ transitions) is ignorable for the magnetic field strength of this helicon source (< 800 G).²¹ The fluorescence radiation is collected at 90° with respect to the laser beam by optics (similar with that described previously) mounted on a platform capable of two-dimensional motion in the plane perpendicular to the collection optics line-of-sight. The range of motion is sufficient to investigate approximately ± 3 cm of the plasma column in the radial direction along the laser beam. The LIF signal is accumulated during each plasma pulse (and dwell interval) at a digitation rate of 5 kHz and averaged over 100

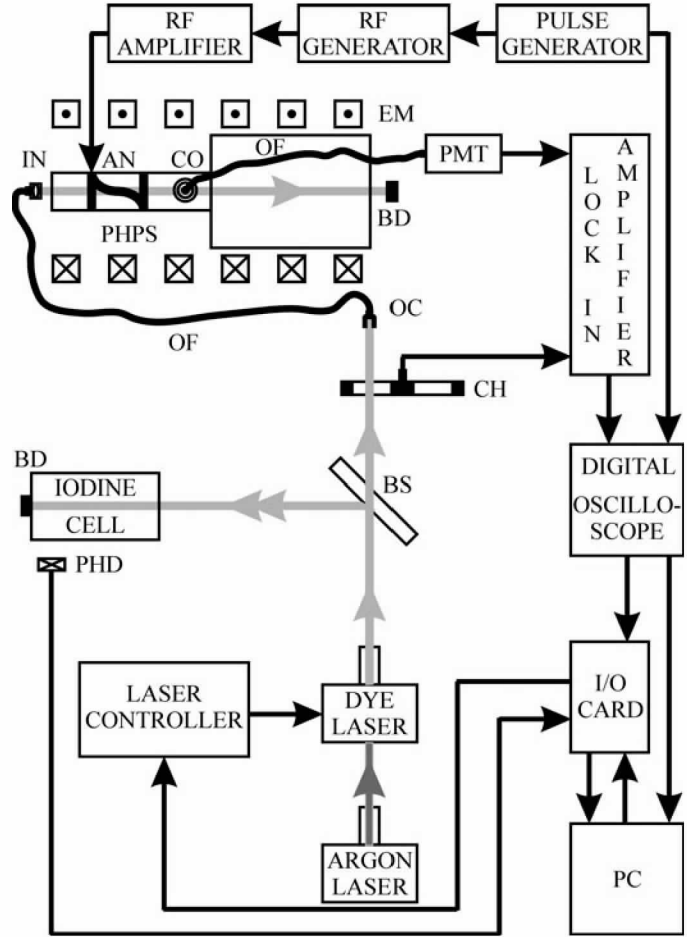


Figure 1. Experimental set-up for time resolved LIF diagnostic: PHPS–pulsed helicon plasma source, IN–injection optics, AN–antenna, CO–collection optics, BD–beam dump, EM–electromagnets, PMT–photomultiplier tube, OF–optical fiber, OC–optical coupler, CH–mechanical chopper, PHD–photo diode, BS– beam splitter.

cycles. After each averaged time series is acquired, the laser is tuned to a new wavelength. Typically 30 wavelengths over a laser frequency range of 8 GHz are needed to obtain reliable ion distribution function measurements. A typical rf pulse waveform is shown in Fig 2. Superposed in Fig. 2 are time resolved LIF measurements for 5 distinct wavelengths processed by the lock-in amplifier, and averaged over 100 plasma pulses. The appearance of a significant LIF signal as the laser wavelength is tuned through the absorption line is evident in the time series data. After subtraction of the time-dependent background signal, the LIF signal to noise is better than 10:1. For the data shown in Fig. 2, the lock-in time constant was 1 ms and the lock-in output signal was updated at a rate of 512 Hz, thereby limiting the time resolution of the data in Fig. 2 to 1.95 ms. Close inspection of Fig. 2 would show the roughly 2 ms time lag in the LIF waveform relative to the plasma pulse initiation due to the 512 Hz update rate of the lock-in.

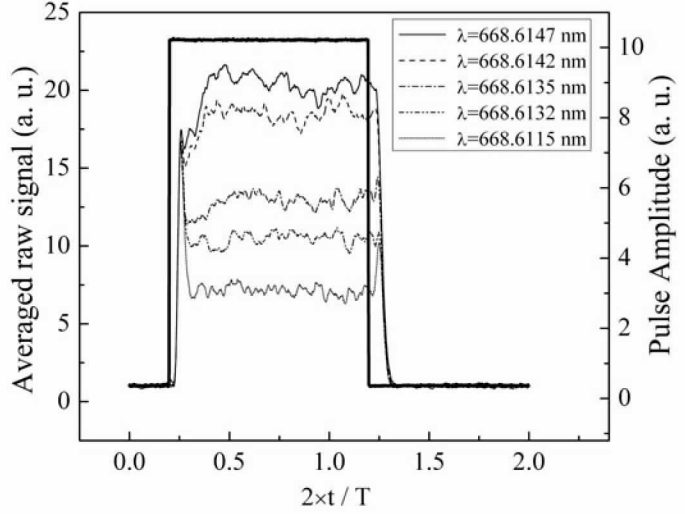


Figure 2. The rf pulse (full thick line) and LIF signal from the lock-in amplifier for 5 distinct wavelengths.

IV. Temporal behavior of parallel and perpendicular ivdfs

Recent numerical modeling has predicted,²² and experimental investigations demonstrated,⁶ that in a steady-state helicon generated expanding argon plasma, near the junction between the helicon source and the diffusion chamber, two ion populations coexist: a slow moving group and a fast moving group. The first group represents a background population, which flows at moderate velocities downstream toward diffusion chamber. The second group arises due to the formation in the expansion region, at pressures below a threshold value, typically 1 – 2 mTorr, of a current free electric double layer (EDL). The length of space charge separation, i.e., the EDL thickness is from few tens to a few hundred Debye lengths, λ_D ($\lambda_D = (\epsilon_0 k_B T_e / e^2 n_e)^{1/2}$, where ϵ_0 stands for dielectric permittivity of the vacuum). Depending on the EDL strength ($e \Phi / k_B T_e$) the ions that pass downstream through the EDL are accelerated to velocities above the ion sound speed c_s ($c_s = (\gamma k_B T_e / m_i)^{1/2}$, where m_i stands for ion mass and γ is assumed 1 for isothermal expansion). The simulations suggest that the EDL formation is triggered by the rapid decrease in electron density that occurs because of the strongly divergent magnetic field. The evolution of the parallel ivdf during the rf pulse in HELIX-LEIA is shown in Fig. 3 for a 50% duty cycle, 5 Hz pulsed discharge. The pressure was 0.9 mTorr, magnetic field 750 Gauss in HELIX and zero in LEIA, rf driving frequency 9.5 MHz, and the input power was 800 W. As a first step, the ivdf measurements in the pulsed plasma were compared with corresponding LIF measurements in steady-state plasma. To have similar operational plasma parameters, the pressure, magnetic field strength, input power, and rf driving frequency were held constant. Furthermore, once the rf matching network was tuned for steady-state operation and the ivdf measurements obtained, the discharge was switched to pulsed mode without changing the settings of the matching network or the amplitude of the rf source. Under these conditions and for a long pulse “on/off” interval (100 ms), we expected that the ivdf would evolve during the pulse to a final state similar to the ivdf measurements in steady state. Previous probe and LIF measurements in a variety of helicon sources indicates that the EDL forms on the helicon source side of the helicon source – diffusion chamber junction, where the gradient of the magnetic field is maximum. Depending on operational parameters, in HELIX-LEIA, the EDL was observed 0 – 20 cm upstream the junction.⁶ Thus, the LIF sample volume was in the EDL in HELIX (4 cm inside the helicon source). Due to large random fluctuations in the emission signal during the first 20 ms of the discharge, most likely associated with bursts of ion production during breakdown that saturate the lock-in amplifier, the exact moment of the formation of the fast group of ions can not be determined from these measurements. However, two ion groups are clearly visible in the 3D graph once the signal-to-noise of the LIF data improves: the fast group with flow speeds between 4.2 and 5.2 km/s and the slow group with speeds of 2.2 – 3.4 km/s. That the first group is created by drift from a region of higher potential of the EDL and the slow group represents ions produced by local ionization and/or thermalization of the fast ions by charge exchange and elastic collisions can be seen by comparing the respective flow speeds to the ion sound speed. For an electron temperature of $T_e = 9$ eV, as

measured with rf compensated Langmuir probe, $c_s = 4.6$ km/s, and therefore the fast ions are flowing along the magnetic field at a speed of 0.9 – 1.1 Mach. The slow group is flowing subsonically at 0.5 – 0.7 Mach. The ion temperature inferred from FWHMs of the two population distributions is another indication that fast group is formed by passing through the EDL while the slow group is generated locally. The fast ion group has a beamlike distribution function with a small energy spread ($T_{if} \approx 0.18$ eV), constant during the pulse, while the slow group ion temperature reaches $T_{is} \approx 0.5$ eV at the end of the pulse, consistent with ion heating due to charge exchange and elastic collisions.²³ As the discharge evolves, both flow speeds continue to increase. Two possible explanations are either that the EDL is moving past the measurement location or that the EDL is not fully developed and does not reach steady state during the 100 ms pulse “on” interval. The first possibility is unlikely since: (a) a moving EDL similar to those observed in collisionless expanding plasmas²⁴ would propagate with the ion acoustic velocity, yielding a transit time across our system on the order of ≈ 300 μ s – more than two orders of magnitude shorter than the rf pulse. Such short time scale phenomena are undetectable with the time resolution achieved in these experiments. However, since those experiments demonstrated that the EDL stagnates after 200 – 300 μ s,²⁵ these observations of continued evolution of the flow speed during the 100 ms pulse are inconsistent with a moving, collisionless EDL. (b) the LIF amplitude (proportional with the square of ion density)⁵ of the slow ion population is constant during the pulse – implying a constant ionization rate at the observation location – inconsistent with a moving EDL since quasineutrality requires a larger ion density on the high potential of a EDL and therefore the ion density would increase in time; (c) For Ar^+ energies between 1.5 eV (slow group) and 5.6 eV (fast group), the total momentum transfer cross-section for Ar^+ - Ar collisions including charge exchange and elastic collisions is about $\sigma = 1.5 \times 10^{-14}$ cm². This cross-section yields an ion mean free pass λ_{mfp} of about 4.5 cm. Additional parallel ivdf measurements were performed as function of axial location at fixed plasmas parameters of 1.3 mTorr, 800 W, and for the same magnetic configuration. Fast ion group was rapidly attenuated over a distance of few mean free paths, i.e., the square root of amplitude of the fast ion population LIF signal to the slow ion population decreased from 2 in the EDL to about 0.5 at 35 cm downstream of the EDL.

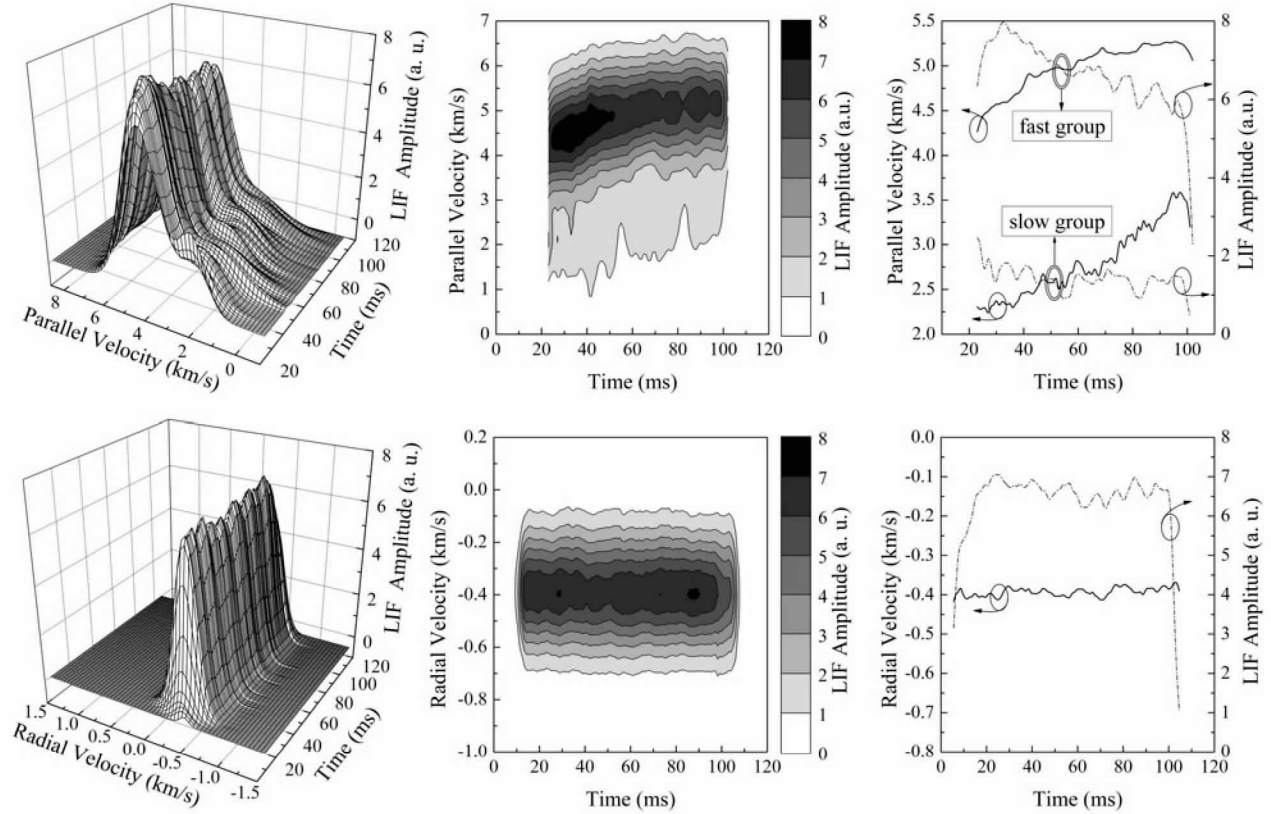


Figure 3. Temporal evolution of ivdf. Top row – parallel ivdfs in HELIX – LEIA machine; Bottom row – perpendicular ivdfs in BMW machine. Left – 3D map surface plot; middle – contour plot in (v, t) plane; right – peak ion flow velocity (full line) and LIF signal amplitude (chain line).

The second possibility, that the EDL is not yet fully formed after 100 ms, is more likely given that in steady-state operation the speed of the fast ion group is about 7.8 km/s (1.7 Mach), much higher than the flow speed observed at the end of the 100 ms pulse. Such high ion speeds correspond to a potential drop across the EDL of $\Phi \approx 13$ V, more than double than what is observed at the end of the pulse. On the low speed side of the slow group portion of the ivdf, the distribution has a long, non-Maxwellian tail – consistent with creation of the slow ion group in the EDL and subsequent acceleration by a fraction of the total potential across the EDL. Note also that the nearly identical rates of speed increase, ≈ 14 m/s², for both the slow and fast ion groups during the pulse is consistent with an increasing potential drop across the EDL.

Applying the electron flux balance equation to the boundary of two different plasmas and assuming that the generated thermoelectric field vanishes at the foot of the EDL, Chan *et al*²⁶ found that the strength of the EDL that forms between two plasmas obeys

$$\exp(-e\Phi / k_B T_{eH}) = n_{eL} T_{eL}^{3/2} / n_{eH} T_{eH}^{3/2}, \quad (3)$$

where the subscripts *H* and *L* correspond to the high and low potential sides of the EDL, respectively. Based on their model, a qualitative picture of EDL temporal evolution can be formulated as follows. Once the EDL forms, the flow of ions and electrons upstream and downstream, respectively, is limited. The positive and negative space charge on high potential side and low potential side of the EDL will build up and the EDL strength will increase until equilibrium is reached, i.e., when the number of energetic electrons from the tail of the electron distribution function on the high potential side able to overcome the potential barrier balances the number of electrons crossing the EDL from the low potential side. Therefore, downstream of the EDL we observe that the speed of the fast ion population (ions accelerated through upstream presheath and EDL) increases during the pulse since the space charge and consequently the potential drop across the EDL is increasing. Since our observation point is in the EDL, the slow ion population can be associated with the local ionization process in the strengthening EDL and is accelerated by only a portion of the total potential drop across the EDL. For our plasma parameters, $T_{eH} = 9$ eV, $n_{eH} = 2 \times 10^{11}$ cm⁻³ in HELIX and $T_{eL} = 6$ eV, $n_{eL} = 5 \times 10^{10}$ cm⁻³ in LEIA⁵, Eq.(3) predicts a steady-state potential drop of ≈ 18 V, which is in reasonable agreement with the ≈ 13 V potential drop estimated from the flow velocity data.

Shown in the second row of Fig. 3 is the evolution of the perpendicular ivdf in the BWX machine for the same pulse length and duty cycle as for the parallel measurements. The perpendicular ivdf evolution was obtained by stepping the laser around the absorption wavelength 668.6138 nm and averaging over 100 pulses. The collection optics was 20 cm downstream of the aluminum plate at the source/chamber junction and viewed plasma 2 cm from the source axis. The pressure was 1 mTorr, magnetic field 260 Gauss, and rf driving frequency 13.56 MHz. Since the lower rf power of 300 W yielded a quieter discharge breakdown phase, good LIF signal was obtained after the first 4 ms of the pulse. The shift in frequency of the peak LIF emission frequency was relatively constant throughout the discharge. The inferred values of the bulk ion speed show a modest outward ion flow (radially outward) of about 400 m/s and no evidence of ion acceleration and electric field structures in radial direction. The perpendicular ion temperature calculated from Gaussian fits to the measured ivdf is a nearly constant 0.05 eV, yielding an ion thermal speed of 400 m/s – comparable to the measured bulk radial diffusion speed. LIF measurements obtained during the plasma afterglow indicate that the rate of decrease of the perpendicular ion temperature is much smaller than the rate of decrease in the LIF intensity. Thus, it is possible that afterglow measurements could be used to investigate both the energy and plasma confinement times of helicon source plasmas.

V. Conclusion

In summary, by using a laser induced fluorescence diagnostic technique with a time resolution of 1 ms, we have investigated the temporal evolution of the ion velocity distribution function in two different pulsed helicon discharges. The parallel ivdf measurements confirm that in the expansion region of a helicon generated plasma, for certain operational conditions, two ion populations exists. A fast ion group having a beamlike distribution, accelerated to supersonic speed by an electric double layer and a slow moving group formed by local ionization. Analysis of the ivdf temporal evolution shows that in a collisional plasma, although it forms within 20 ms, the double layer has not reached a steady state by 100 ms into the rf pulse. This is in contrast to EDLs created by plasma expansion into a vacuum, where steady-state EDLs were observed after only a few hundred microseconds. In a qualitatively similar helicon source, although the EDL appeared in about 100 μ s, a steady-state EDL also required 100 – 200 ms.¹² Measurements of perpendicular ivdf evolution in a pulsed plasma show little change throughout the pulse. Modest and steady radially outward flows on the order of the ion thermal speed were observed.

For plasma thruster concepts with magnetic nozzles, using a pulsed operation instead steady-state may resolve the contradicting requirements of efficient plasma acceleration and plasma detachment. Since detachment of the plasma flow from the vacuum magnetic field lines can occur only after the kinetic energy density of the plasma flow exceeds the energy density of the diverging magnetic field of the nozzle, pulses with pulse “on” times just long enough to fulfill the above condition might be an efficient means of generating high energy density plasmas that then detach.

Acknowledgments

This work was supported by U.S. Department of Energy EPSCoR Laboratory Partnership Program grant ER45849 and by NSF grant PHY-0315356.

References

- ¹ Glover, T. W., Chang Diaz F. R., Squire, J. P., Jacobson, V. P., Chavers, D. G., and Carter, M. D., “Principal VASIMR Results and Present Objectives”, 2005, *AIP Conference Proceedings*, Vol. 746, No. 1, pp. 976-982
- ² Spektor, R. and Choueiri, E. Y., “Ion acceleration by beating electrostatic waves: Domain of allowed acceleration”, 2004, *Physical Review E*, Vol. 69, No. 4, pp. 046402-1 – 046402-9
- ³ Cohen, S. A., Siefert, N. S., Stange, S., Scime, E. E., Boivin, R. F., and Levinton, F., “Ion acceleration in plasmas emerging from a helicon-heated magnetic-mirror device”, 2003, *Physics of Plasmas*, Vol. 10, No. 6, pp. 2593-2598
- ⁴ Charles, C. and Boswell, R. W., “Current-free double-layer formation in a high-density helicon discharge”, 2003, *Applied Physics Letters*, Vol. 82, No. 9, pp. 1356-1258
- ⁵ Sun, X., Biloiu, C., Hardin, R., and Scime, E., “Parallel velocity and temperature of argon ions in an expanding, helicon source driven plasma”, 2004, *Plasma Sources Science and Technology*, Vol.13, No. 3, pp. 359-370
- ⁶ Sun, X., Keese, A., Biloiu, C., Scime, E., Meige, A., Charles, C., and Boswell, R. W., 2005, “Observations of Ion-Beam Formation in a Current-Free Double Layer”, *Physical Review Letters*, Vol. 95, No. 2, pp. 025004-1 – 025004-4
- ⁷ Winglee, R. M., Ziemba, T., Euripides, P., and Slough, J., “Magnetic inflation produced by the Mini-Magnetospheric Propulsion (M2P2) prototype”, 2002, *AIP Conference Proceedings*, Vol. 608, No. 1, pp. 433-440
- ⁸ Ziemba, T., Slough, J., and Winglee, R. M., “High Power Helicon Propulsion Experiments”, 2005, *AIP Conference Proceedings*, Vol. 746, No. 1, pp. 965-975
- ⁹ Scime, E., Biloiu, C., Compton, C., Doss, F., Ventura, D., Heard, J., Choueiri, E., and Spektor, R., “Laser induced fluorescence in a pulsed argon plasma”, 2005, *Review of Scientific Instruments*, Vol. 76, No. 2, pp. 026107-1 – 026107-1
- ¹⁰ Spektor, R., and Choueiri, E., “An Experiment for Studying Ion Acceleration by Beating Electrostatic Waves”, *Proceedings of 38th Joint Propulsion Conference*, AIAA paper 2002-3801, July 2002
- ¹¹ Spektor, R., and Choueiri, E., “Excitation and Propagation of Electrostatic Ion Cyclotron Waves in rf-Sustained Plasmas of Interest to Propulsion Research”, *Proceedings of 40th Joint Propulsion Conference*, paper 2004-4095, July 2004
- ¹² Charles, C. and Boswell, R. W., “Time-development of current-free double-layer”, 2004, *Physics of Plasmas*, Vol. 11, No. 8, pp. 3808-3812
- ¹³ Sarfaty, M., De Souza-Machado, S., and Skiff, F., “Direct determination of ion waves field in a hot magnetized and weakly collisional plasma”, 1996, *Physics of Plasmas*, Vol. 3, No. 12, pp. 4316-4324
- ¹⁴ Biloiu, C., Scime, E., Sun, X., and McGeehan, B., “Scanning internal probe for plasma particle, fluctuation, and LIF tomographic measurements”, 2004, *Review of Scientific Instruments*, Vol. 75, No.10, pp. 4296-4298
- ¹⁵ Scime, E., Boivin, R., Kline, J., and Balkey, M., “Microwave interferometer for steady-state plasmas”, 2001, *Review of Scientific Instruments*, Vol. 72, No. 3, pp. 1672-1676
- ¹⁶ Jackson, G., Lewis, C., Doorn, S., Majidi, V., and King, F., “Spectral, spatial and temporal characteristics of a millisecond pulsed glow discharge: metastable argon atom production”, 2001, *Spectrochimica Acta B*, Vol. 56, No. 12, pp. 2449-2464
- ¹⁷ Bachet, G., Cherigier, L., Arnas-Capeau, C., Doveil, F., and Stern, R. A., “Laser Induced Fluorescence of Ion Velocity Distribution Function Modifications Induced by Electrostatic Ion Shock Waves”, *Journal of Physics III France*, Vol. 6, No. 9, pp. 1157-1165
- ¹⁸ Pelissier, B., and Sadeghi, N., “Time-resolved pulse-counting lock-in detection of laser induced fluorescence in the presence of a strong background population”, 1996, *Review of Scientific Instruments*, Vol. 67, No. 10, pp. 3405-3410
- ¹⁹ Bachet, G., Skiff, F., Dindelegan, M., Doveil, F., and Stern, R. A., “Laser-induced Fluorescence Observation of Self-Organized Ion Structures Induced by Electrostatic Perturbations”, 1998, *Physical Review Letters*, Vol. 80, No. 15, pp. 3260-3263
- ²⁰ Severn, G. D., Edrich, D. A., and McWilliams, R., “Argon ion laser-induced fluorescence with diode lasers”, 1998, *Review of Scientific Instruments*, Vol. 69, No. 1, pp. 10-15
- ²¹ Boivin, R. F. and Scime, E. E., “Laser induced fluorescence in Ar and He plasmas with a tunable diode laser”, 2003, *Review of Scientific Instruments*, Vol. 74, No. 10, pp. 4352-4360
- ²² Meige, A., Boswell, R. W., Charles, C., and Turner, M., “One-dimensional particle-in-cell simulation of a current-free double layer in an expanding plasma”, 2005, *Physics of Plasmas*, Vol. 12, No. 5, pp. 052317-1 – 052317-10
- ²³ Anderegg, F., Stern, R. A., Skiff, F., Hammel, B. A., Tran, M. Q., Paris, P. J., and Kohler, P., “Ion Heating Due to Rotation and Collision in Magnetized Plasma”, 1986, *Physical Review Letters*, Vol. 57, No. 3, pp. 329-332
- ²⁴ Hairapetian, G. and Stenzel, R., “Expansion of a Two-Electron-Population Plasma into Vacuum”, 1988, *Physical Review Letters*, Vol. 61, No. 14, pp. 1607-1610
- ²⁵ Hairapetian, G. and Stenzel, R., “Particle dynamics and current-free double layers in an expanding collisionless, two-electron-population plasma”, 1991, *Physics of Fluids B*, Vol. 3, No. 4, pp. 899-914
- ²⁶ Chan, C., Hershkovitz, N., and Lonngren, K., “Electron temperature differences and double layers”, 1983, *Physics of Fluids*, Vol. 26, No. 6, pp. 1587-1595